Metallic iron limits silicate hydration in Earth's transition zone

Feng Zhu[a,1,2], Jie Li[a], Jiachao Liu[a], Junjie Dong[a,3], and Zhenxian Liu[b]

[a]Earth and Environmental Sciences, University of Michigan, Ann Arbor, MI 48109; and [b]Department of Physics, University of Illinois at Chicago, Chicago, IL 60607

Edited by Ho-Kwang Mao, Center for High Pressure Science and Technology Advanced Research, Shanghai, China, and approved September 27, 2019 (received for review May 21, 2019)

The Earth's mantle transition zone (MTZ) is often considered an internal reservoir for water because its major minerals wadsleyite and ringwoodite can store several oceans of structural water. Whether it is a hydrous layer or an empty reservoir is still under debate. Previous studies suggested the MTZ may be saturated with iron metal. Here we show that metallic iron reacts with hydrous wadsleyite under the pressure and temperature conditions of the MTZ to form iron hydride or molecular hydrogen and silicate with less than tens of parts per million (ppm) water, implying that water enrichment is incompatible with iron saturation in the MTZ. With the current estimate of water flux to the MTZ, the iron metal preserved from early Earth could transform a significant fraction of subducted water into reduced hydrogen species, thus limiting the hydration of silicates in the bulk MTZ. Meanwhile, the MTZ would become gradually oxidized and metal depleted. As a result, water-rich region can still exist near modern active slabs where iron metal was consumed by reaction with subducted water. Heterogeneous water distribution resolves the apparent contradiction between the extreme water enrichment indicated by the occurrence of hydrous ringwoodite and ice VII in superdeep diamonds and the relatively low water content in bulk MTZ silicates inferred from electrical conductivity studies.

mantle transition zone | water budget | redox reaction | mantle oxidation state | deep hydrogen cycle

Water can profoundly influence the properties and behaviors of silicates and oxides, and thus the role of water in mantle chemistry and dynamics has attracted extensive studies for decades. In particular, the mantle transition zone (MTZ) has been considered a potential water reservoir with the ability to hold several oceans of water (1), because its major phases wadsleyite and ringwoodite can incorporate up to 2 to 3 wt % water in their structures (2). Whether the MTZ is a hydrous layer or just an empty reservoir, however, remains highly controversial. Current estimates of water content in the MTZ silicates from geophysical, geochemical, and petrological studies vary from nearly 0 to 2 wt % (3–12), whereas regional hydration associated with subduction has been inferred by numerous geophysical measurements (10, 13–15).

Previous studies predicted the presence of metallic iron in the deep mantle due to disproportionation of ferrous iron (Fe^{2+}) into iron metal (Fe^0) and ferric iron (Fe^{3+}) in silicates (16–19). In the MTZ, such disproportionation may produce ~0.14 wt % iron from majorite garnet, and smaller amounts from wadsleyite and ringwoodite (18, 20). Native iron and iron alloy in some superdeep diamonds were interpreted as possible evidences for a reduced MTZ (21, 22). On the other hand, iron metal was found to react with water or hydrous melt to form oxide and hydride (23–26), suggesting that metal saturation may be incompatible with a hydrous MTZ. It is unknown, however, if iron can react directly with the structural water in nominally anhydrous minerals such as hydrous wadsleyite and hydrous ringwoodite. Here, we conduct high-pressure and -temperature experiments to investigate the stability of hydrous wadsleyite in the presence of iron metal and explore the implications for the oxidation state as well as the concentration and distribution of hydrogen in the MTZ.

Results

Experiments were conducted at 15 GPa and 1,400 °C using multianvil apparatus (MA), corresponding to the conditions in the upper part of the MTZ (27) (*SI Appendix*, Table S1 and Fig. S1). Reaction between iron and synthetic iron-free hydrous wadsleyite (*SI Appendix*, Fig. S2) produced wadsleyite and ringwoodite $(Mg,Fe)_2SiO_4$, a small amount of ferropericlase (Mg,Fe)O, iron spheres, and iron-rich domains with the texture of partial melt (Fig. 1 *A* and *B*). Similar products were observed in comparison experiments which started with free water, iron, and Mg_2SiO_4 (*SI Appendix*, Figs. S3–S5). The reaction between iron and hydrous wadsleyite can be described as

$$(2+x)Fe + Mg_{2-x}H_{2x}SiO_4 = Mg_{2-x}Fe_xSiO_4 + 2FeH_x. \quad [1]$$

$(Mg,Fe)_2SiO_4$ nearest the iron foil was transformed from wadsleyite into ringwoodite due to iron enrichment (28). The small iron spheres in the reaction zone are inferred as the decomposition products of molten FeH_x droplets. (Mg,Fe)O and hydrous melt are not direct products in reaction **1** and their formations are possibly due to moisture and temperature uncertainties in the experiments (*SI Appendix*, Text S1).

Fourier-transform infrared (FTIR) line scans were performed on the experimental products to evaluate the distribution of water content (Fig. 1*C* and *SI Appendix*, Fig. S6). The spectrum

Significance

Some studies suggested that the Earth's mantle transition zone (MTZ) consists of hydrous silicates while others proposed that it contains iron metal. Here we show that the metallic iron dehydrates hydrous silicates at MTZ conditions, implying that global hydration of silicates and metal saturation are incompatible. Comparing iron production in and water injection to the MTZ, we found that the hydration of MTZ silicates is likely limited to <0.1 wt %, while large amount of the hydrogen can be stored as iron hydride and hydrogen fluid instead. Water-rich domains may still exist near the modern active subducted slabs. Our finding connects the water content to the oxidation state of the MTZ, thus providing a different perspective on volatile cycles in the mantle.

Author contributions: F.Z. and J. Li designed research; F.Z., J. Li, J. Liu, J.D., and Z.L. performed research; F.Z., J. Li, and Z.L. analyzed data; and F.Z. and J. Li wrote the paper.

The authors declare no competing interest.

This article is a PNAS Direct Submission.

[1]To whom correspondence may be addressed. Email: fzhuum@umich.edu.

[2]Present address: Hawai'i Institute of Geophysics and Planetology, School of Ocean and Earth Science and Technology, University of Hawai'i at Mānoa, Honolulu, HI 96822.

[3]Present address: Department of Earth and Planetary Sciences, Harvard University, Cambridge, MA 02138.

This article contains supporting information online at www.pnas.org/lookup/suppl/doi:10.1073/pnas.1908716116/-/DCSupplemental.

First published October 21, 2019.

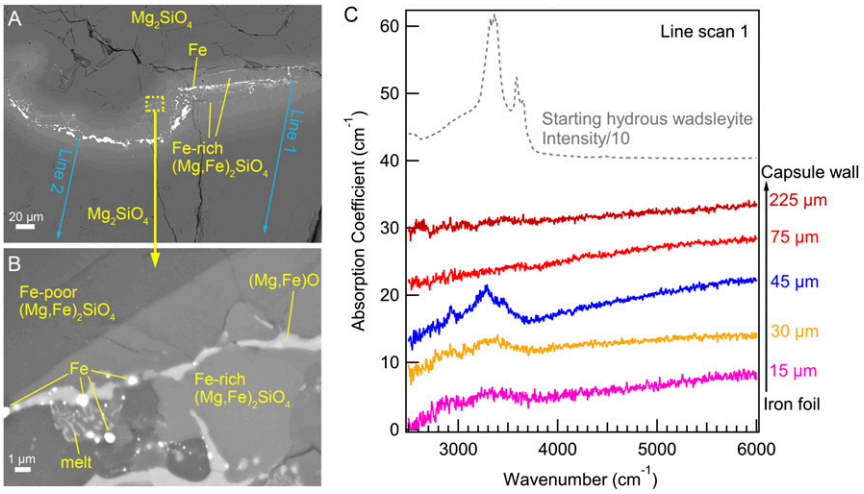

Fig. 1. Back-scattered electron (BSE) image and FTIR spectra of the quenched products from experiment M072816 where iron and hydrous wadsleyite equilibrated at 15 GPa and 1,400 °C for 2 h. (*A*) A reaction zone (light gray) composed of mainly $(Mg,Fe)_2SiO_4$ formed between iron (white) and wadsleyite Mg_2SiO_4 (dark gray). (*B*) An area in the reaction zone (yellow dashed box) containing Fe spheres (white), which are interpreted as the decomposition products of molten FeH_x droplets. (*C*) FTIR absorption spectra along the line scans of the run products in comparison with the hydrous wadsleyite starting material (line 1 in Fig. 1*A*). A 10-fold reduction was applied to the intensity of starting hydrous wadsleyite which contains ~0.90 wt % water (dashed gray line) (29). Near the iron foil (15 and 30 μm), the spectra showed almost no detectable OH^- bands, corresponding to less than tens of ppm water. Slightly away from iron foil (45 μm), several OH^- bands appeared which correspond to hydrous phases and fluid preserved from reaction due to limited diffusion. Away from the reaction zone (75 and 225 μm), the OH^- signal disappeared again. The original spectra without background treatment and the spectra of line scan 2 are found in *SI Appendix*, Fig. S6.

nearest the iron foil showed almost no OH^- band, indicating the reaction dehydrated the wadsleyite with ~0.90 wt % water to nearly anhydrous silicate containing less than tens of ppm water (29). Regions slightly away from iron foil still preserved a small amount of water in the form of hydrous fluid and phases, which did not react with iron foil completely possibly due to limited diffusion rate (*SI Appendix*, Text S2). Away from the reaction zone where dry Fo100 powder was initially placed, the OH^- signal was invisible again.

Besides the FTIR measurements, reduction of OH^- to H^0 and oxidation of Fe^0 to Fe^{2+} can also be inferred from the Fe^{2+} enrichment in silicates, because without an oxidizing agent such as structural or free water, metallic iron cannot react with iron-free wadsleyite. However, moisture in sample and pressure medium is inevitable, which may also be able to oxidize the metallic iron. Therefore, a nominally anhydrous run was performed with only iron and anhydrous Mg_2SiO_4 as starting materials to provide a baseline for the effect of moisture. In the nominally anhydrous experiment, we observed a narrow reaction zone which contains much less Fe^{2+} than those in hydrous experiments (*SI Appendix*, Figs. S3 and S7), proving that hydrous wadsleyite or free water was the main cause for the observed large-scale oxidation of metallic iron in hydrous experiments. Our results are consistent with the previous study showing that H prefers iron metal to ringwoodite (25), although a recent research suggests H is lithophile instead of siderophile at 5 to 20 GPa (30), which has been questioned (31) and calls for further investigation (*SI Appendix*, Text S3).

In an experiment with excess water, we further extended the heating duration to 48 h. No metallic Fe was found in the reaction products (*SI Appendix*, Fig. S8), indicating that FeH_x is further oxidized to FeO to produce hydrogen at 15 GPa and 1,400 °C through the following reaction:

$$FeH_x + 2H^+ = Fe^{2+} + (x/2+1)H_2. \quad [2]$$

In a simple system with $FeH_x + H_2O$, our laser-heated diamond-anvil cell (DAC) experiments also confirmed similar reaction (*SI Appendix*, Fig. S9).

As no kinetic hindrance was observed in the reaction between iron metal and structurally bonded water in wadsleyite, we posit that metallic iron can reduce subducted water regardless of its transport history. It implies that iron metal must be consumed before the silicate in a region can be hydrated to more than tens of ppm of water. In other words, a hydrous region is necessarily oxidized and metal free, whereas a metal-saturated region must be nearly anhydrous.

Estimates on the amount of water injected to MTZ may be used to evaluate its current water content and oxidation state. The MTZ silicates likely started with less than 0.1 wt % water in the Archean Eon because it was 200 to 400 °C hotter and therefore the maximum water storage capacity of wadsleyite and ringwoodite was below 0.1 wt % (*SI Appendix*, Text S4). We thus consider the later delivery by subduction as the major water source. The initial concentration of metallic iron before 4 Ga was estimated at 0.14 wt % (18), corresponding to a consumption capacity of 0.05 to 0.14 ocean of water by reaction, depending on whether FeH or H_2 is produced (*SI Appendix*, Text S5). We first consider an end-member case where subducted water and iron metal equilibrate globally (Fig. 2*A*). If the water input is below the consumption capacity of metallic iron, MTZ silicates would remain dry and the hydrogen would be stored in a reduced form; If the water input exceeds this consumption capacity, the MTZ would be oxidized to above the iron-wüstite buffer with metallic iron fully consumed, and the silicates can be hydrated with further water injection.

Two estimates of water fluxes were used to calculate the total water input (*SI Appendix*, Table S2) (32–34). The lower estimate of 0.074 ocean mass input in 4 Ga falls between the water consumption capacity of producing FeH and H_2. If the reaction produces mainly H_2, then all of the injected water would be consumed, leaving the MTZ silicates nearly dry with half of the iron metal preserved; if the reaction produces mainly FeH, the bulk MTZ would end up free of iron metal with an average of 170 ppm water in wadsleyite and ringwoodite. The higher estimate of total water input at 0.2 ocean mass exceeds the maximum water consumption capacity of iron in the MTZ; hence, there would be enough water to react with all of the iron metal

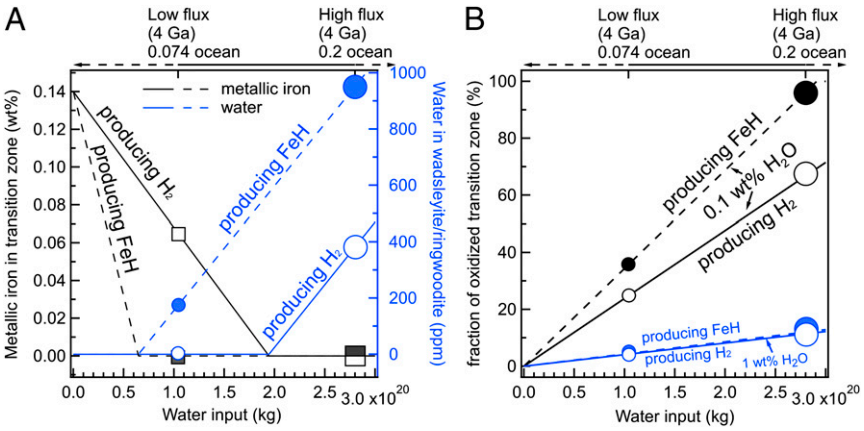

Fig. 2. Oxidation and hydration of MTZ by water from subducted slabs. (*A*) Global equilibrium model, assuming vigorous mantle convection. In this case, all of the metallic iron can react with all of the injected water, and the excess iron or water distributes evenly in the whole MTZ. The black and blue lines correspond to the iron and water concentration in the MTZ as a function of water input, respectively. Solid and dashed lines assume producing H_2 and FeH in reaction, respectively. Small and large symbols (square for iron and circle for water) represent the results of two estimated water flux at 2.6×10^{10} kg/y (32, 33) (low flux) and 7×10^{10} kg/y (34) (high flux), respectively. (*B*) Local hydration model, assuming that the mantle convection is too sluggish to allow full equilibrium between iron metal and water. In this case, iron is consumed locally and excess water is retained in silicates before further reacting with iron in other places. Lines and symbols are the same as in *A*, except that the blue and black lines represent the fraction of oxidized and hydrous MTZ as a function of water input when 1 wt % and 0.1 wt % is retained locally by hydrous wadsleyite and ringwoodite, respectively. The water flux may be below or above the estimated range as indicated by dashed arrows (*SI Appendix*, Text S6). Data are found in *SI Appendix*, Table S3.

and produce an MTZ that is metal-free with an average water concentration of 380 to 950 ppm in wadsleyite and ringwoodite (Fig. 2*A* and *SI Appendix*, Table S3).

In the global equilibrium model, the injected water may be able to fully consume the metallic iron, implying that MTZ could have become significantly more oxidized with time. But, in most scenarios the remaining water can barely hydrate the MTZ silicates to an average water concentration of 0.1 wt %. The water consumption capacity of iron and subducted water flux both have large uncertainties (*SI Appendix*, Text S6); hence, the possibility of a more hydrous MTZ cannot be ruled out. However, hydration of the MTZ silicates is likely limited or influenced by the presence of metallic iron, despite their large water storage capacity. Meanwhile, reduced hydrogen species such as iron hydride and hydrogen fluids can be important hydrogen hosts other than silicates. More precise data on water flux throughout the Earth's history will be crucial to determine the hydrogen species, contents, and oxidation states of MTZ jointly.

The global equilibrium model assumes the injected water can access all of the metallic iron in the MTZ. However, heterogeneity would exist if the reaction is limited by slow water diffusion and insufficient mantle convection. In the local hydration model, we assume the other extreme case that after iron metal is locally consumed, water is stored and held by hydrous silicates in the oxidized region throughout Earth's history (Figs. 2*B* and 3). With 0.074 to 0.2 ocean water input, if wadsleyite and ringwoodite acquire ~1 wt % water to reach their full storage capacities at the present mantle temperature, then only 4 to 12% of the MTZ would be oxidized and hydrated, and the bulk MTZ would remain dry and saturated with iron metal. If the retained water decreases to 0.1 wt %, the fraction of oxidation extends to 70 to 100% of MTZ with high flux, which goes back to the global equilibrium model.

Over geological time, water has been injected at numerous subduction sites. Through diffusion and mantle convection, a large fraction of the injected water from ancient slabs could have reached and reacted with the metallic iron globally. Modern active slabs, on the other hand, may not have fully equilibrated with the bulk MTZ and therefore hydrous silicates may be locally preserved. Applying the local hydration model to modern active slabs in the past 200 Ma, and the global equilibrium model to ancient slabs subducted between 4 Ga to 200 Ma ago, then only 0.2 to 0.6% of the MTZ could acquire 1 wt % water; the bulk MTZ would contain only 0 to 0.1 wt % water (*SI Appendix*, Table S3).

Discussion

Several lines of evidence support a nearly anhydrous or moderately hydrous bulk MTZ with local water enrichment near active subducted slabs. The electrical conductivity measurements as a sensitive probe to detect water (35) suggest 0 to 0.2 wt % water in bulk MTZ silicates (3, 4, 10), consistent with our estimate of nearly 0 to 0.1 wt % water within uncertainty. It is also close to the recent result 0.22 wt % from sound velocity measurements (5) but significantly lower than the 1 to 2 wt % from viscosity measurements (8), which are also inconsistent with each other and require further examination (*SI Appendix*, Text S7). Local hydration is further indicated by the high-conductivity regions near active oceanic slabs (10) and the low-velocity zones atop 410 km in association with the initiation of Pacific subduction tens of Ma ago (14, 15, 36). The broadening of 410-km discontinuity beneath the Mediterranean region was also attributed to modest hydration of silicates from subducted slabs in the past 190 Ma (13). These mapped contrasts in water concentration may also reflect the history of mantle oxidation by subduction. Furthermore, the origin of superdeep diamonds is considered closely related to the subducted oceanic slabs. The hydrous ringwoodite and ice VII inclusions may thus be associated with local hydration near these slabs (9, 37), and the inclusions containing CH_4 and H_2 associated with metallic iron may be associated with iron hydride and hydrogen fluids resulting from reactions between iron and hydrous phases and fluids at slab-mantle interface (22).

The upper mantle (UM) below 250 km and the lower mantle (LM) were also predicted to contain 0.14 wt % and 1 wt % iron metal, respectively (17, 18). If subducted water was delivered to these mantle layers and could react with iron, then with the high water flux (*SI Appendix*, Table S2), the UM would be oxidized and the constituent silicates would be hydrated to hundreds to thousands of ppm water assuming a global equilibrium, while the silicates in bulk LM probably remain dry because the iron metal can consume up to ~7 ocean water. The water

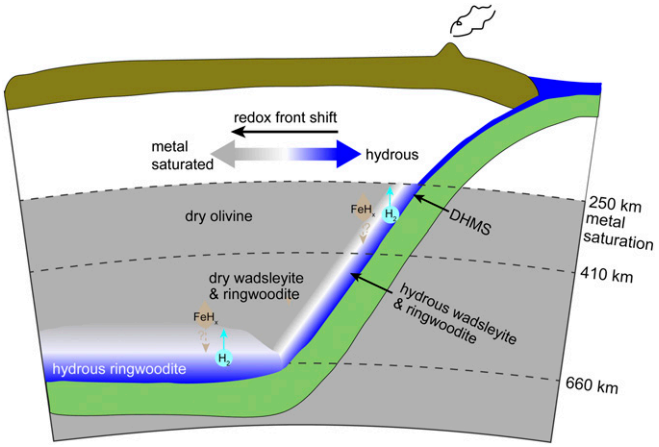

Fig. 3. Cartoon illustration of oxidation and hydration of the MTZ. Water may be carried to a dry and metal-saturated mantle (gray) by oceanic slabs (green) in the form of dense hydrous magnesium silicate (DHMS) phases. Water released from DHMS may be acquired by hydrous wadsleyite or ringwoodite in the mantle. Hydrous phases (including free water and hydrous fluids) react with metallic iron near the slab to form a redox front (white). After local iron metal is consumed, water may be partially retained as structural water in silicates in the metal-free, oxidized region behind redox front (blue). Iron metal in distant regions (gray) is thus preserved from reaction. Continuous water injection would shift the redox front further into the mantle and extend the oxidized and hydrated region from the slab surface into the mantle. In water-rich composition the reaction produces H_2, which rises and brings hydrogen back to shallower depth or the surface. In water-poor composition, the reaction produces FeH_x, which may be trapped in MTZ, or sink and carry hydrogen to greater depths depending on its wetting behavior.

consumption capacity of iron in LM may be further increased if FeO_2H_x instead of FeO is produced from the reaction (38, 39). It indicates that hydrogen transported to the LM may be mostly stored as iron hydride, regardless of the water storage capacity of bridgmanite. Supply of water from the LM to MTZ through equilibrium between silicates is thus not expected. Moreover, a water-enriched MTZ needs to be mostly isolated from the reduced LM during mantle convection to keep its water from reacting with iron metal.

The release of hydrogen fluid or iron hydride from reaction between iron and hydrous phases implies that hydrogen cycle may be decoupled from water cycle which is controlled by the stability of hydrous phases and depth of subduction. If the reaction produces H_2, it may escape to the UM or even the surface through upwelling and convert back to water, with the net effect of oxidizing MTZ by UM Fe^{3+} or possibly the atmospheric oxygen. If the reaction produces FeH_x, it will form a dense melt since its melting temperature is lower than the MTZ geotherm (40). Whether FeH_x melt can stagnate in the MTZ or sink to the LM or the core depends on its wetting behavior, which is still poorly understood and needs further investigation. If FeH_x melt stagnates in the MTZ, with long-term accumulation, it may significantly influence the rheology of MTZ. These pathways for hydrogen could have profound implications for the Earth's volatile cycles and oxidation-state evolution.

Materials and Methods

High-pressure experiments were conducted using the 1,000-ton MA at University of Michigan and at University of Hawai'i at Mānoa with Consortium for Materials Properties Research in Earth Sciences (COMPRES) 10/5 and 8/3 assemblies (41). Sample capsules were made of 0.05-mm-thick gold foil (Goodfellow 99.95%). Starting materials included synthetic forsterite Mg_2SiO_4 (Fo100), synthetic hydrous wadsleyite, and iron powder (Alfa Aesar 10621, 99.998%), iron foils of 0.1 mm thickness (Alfa Aesar 11381, 99.995%) and 0.01 mm thickness (Goodfellow FE000150, 99.850%). The hydrous wadsleyite was synthesized by equilibrating Fo100 powder with deionized water in a gold capsule at 15 GPa and 1,400 °C for 2 h. A transparent crystal was extracted from the center of the capsule and confirmed to be hydrous wadsleyite with Raman and X-ray diffraction (XRD) (*SI Appendix*, Figs. S2 and S5). Brucite was found by Raman in the milky quenched melt near the capsule wall, indicating the following reaction (42):

$$Mg_2SiO_4 + 2xH_2O = Mg_{2-x}H_{2x}SiO_4 + xMg(OH)_2. \quad [3]$$

The starting materials and experimental products were analyzed for texture, chemical composition, and vibrational properties using the JEOL-7800FLV Scanning Electron Microprobe (SEM), CAMECA SX-100 Electron Probe Microanalyzer (EPMA), and Renishaw inVia Raman Microscope at University of Michigan and the SEM in JEOL JXA-8500F EPMA at University of Hawai'i at Mānoa. For SEM and EPMA measurements the samples were coated with carbon. The electron beam was set at 15 keV and 10 nA and focused to 1 μm. Ferrosilite $FeSiO_3$ was used as the standard for Fe quantification in EPMA. The Raman spectra were collected with 532-nm laser source at 5-mW power and 1,800 l/mm gratings. The laser spot was ∼5 μm in diameter.

Synchrotron FTIR absorption spectra were measured at beamline 22-IR-1, National Synchrotron Light Source II (NSLS-II), Brookhaven National Laboratory (BNL). The quenched sample was polished to ∼100-μm thickness and kept on a KBr substrate. To eliminate the influence of water vapor absorption in the O–H stretching vibrational region, all spectra were collected using a Bruker Vertex 80v FTIR spectrometer under vacuum and a dry nitrogen purged Hyperion 2000 IR microscope equipped with a liquid-nitrogen–cooled midband Mercury Cadmium Telluride (MCT) detector. To suppress the fringes caused by the multiple reflections through the sample surfaces, a pair of reflective objectives with 32× magnification and 0.5 numerical aperture were employed. A synchrotron source and a CaF_2 beamsplitter were employed and the aperture was set as ∼15 μm ×15 μm. All spectra include 512 scans at 4-cm^{-1} spectral resolution.

Synchrotron XRD experiments on the synthesized hydrous wadsleyite and iron–water reaction were collected at beamline 13-BM-C and 16-ID-B, respectively, at the Advanced Photon Source (APS), Argonne National Laboratory (ANL). The X-ray wavelengths and beam sizes were 0.434 Å, 12 μm ×18 μm at 13-BM-C and 0.4066 Å, 3.2 μm × 5.8 μm at 16-ID-B, respectively. A symmetric DAC with 300-μm culets was used in the XRD experiment on iron–water reaction. Sample chamber was formed by indenting a 260-μm-thick rhenium gasket to ∼45-μm thickness and then drilling a hole of 180-μm diameter at the center. A 10-μm-thick iron foil (purity 99.85%, Goodfellow) was loaded in the hole filled with deionized water. A ruby sphere was placed near the iron foil as a pressure marker (43). The XRD data were processed using Dioptas (44) and PDIndexer (45) software.

All data needed to support the conclusions are present in the paper or *SI Appendix*.

ACKNOWLEDGMENTS. We thank Hongzhan Fei, Terry Plank, Monika Koch-Müller, Li Zhang, Dave Walker, Marc Hirschmann, Jiuhua Chen, and Eiji Ohtani for fruitful discussion and thank the three reviewers for providing constructive reviews. We thank Bin Chen and Xiaojing Lai for their offer and help on conducting experiments using the resources at University of Hawai'i. This work is partially supported by NSF AST 1344133, NSF EAR 1763189, and NASA NNX15AG54G. FTIR experiments were conducted at beamline 22-IR-1, NSLS-II, BNL. Beamline 22-IR-1 is supported by COMPRES under NSF Cooperative Agreement EAR 1606856 and the US Department of Energy (DOE)/National Nuclear Security Administration (NNSA) (DE-NA-0003858, CDAC). XRD experiments were performed at HPCAT (Sector 16) and GeoSoilEnviroCARS (Sector 13) at APS, a US DOE Office of Science User Facility operated for the DOE Office of Science by ANL under Contract DE-AC02-06CH11357. High Pressure Collaborative Access Team (HPCAT) operations are supported by DOE-NNSA's Office of Experimental Sciences. GeoSoilEnviroCARS is supported by the NSF - Earth Sciences (EAR - 1634415) and DOE- GeoSciences (DE-FG02-94ER14466).

1. J. R. Smyth, A crystallographic model for hydrous wadsleyite (β-Mg_2SiO_4): An ocean in the Earth's interior? *Am. Mineral.* **79**, 1021–1024 (1994).
2. D. Kohlstedt, H. Keppler, D. Rubie, Solubility of water in the α, β and γ phases of $(Mg,Fe)_2SiO_4$. *Contrib. Mineral. Petrol.* **123**, 345–357 (1996).
3. X. Huang, Y. Xu, S. Karato, Water content in the transition zone from electrical conductivity of wadsleyite and ringwoodite. *Nature* **434**, 746–749 (2005).
4. T. Yoshino, G. Manthilake, T. Matsuzaki, T. Katsura, Dry mantle transition zone inferred from the conductivity of wadsleyite and ringwoodite. *Nature* **451**, 326–329 (2008).
5. D. Freitas *et al.*, Experimental evidence supporting a global melt layer at the base of the Earth's upper mantle. *Nat. Commun.* **8**, 2186 (2017).
6. C. Houser, Global seismic data reveal little water in the mantle transition zone. *Earth Planet. Sci. Lett.* **448**, 94–101 (2016).

7. D. Bercovici, S. Karato, Whole-mantle convection and the transition-zone water filter. *Nature* **425**, 39–44 (2003).
8. H. Fei *et al*., A nearly water-saturated mantle transition zone inferred from mineral viscosity. *Sci. Adv.* **3**, e1603024 (2017).
9. D. G. Pearson *et al*., Hydrous mantle transition zone indicated by ringwoodite included within diamond. *Nature* **507**, 221–224 (2014).
10. A. Kelbert, A. Schultz, G. Egbert, Global electromagnetic induction constraints on transition-zone water content variations. *Nature* **460**, 1003–1006 (2009).
11. Z. Mao *et al*., Elasticity of hydrous wadsleyite to 12 GPa: Implications for Earth's transition zone. *Geophys. Res. Lett.* **35**, L21305 (2008).
12. J. Chen, H. Liu, J. Girard, Comparative in situ X-ray diffraction study of San Carlos olivine: Influence of water on the 410 km seismic velocity jump in Earth's mantle. *Am. Mineral.* **96**, 697–702 (2011).
13. M. van der Meijde, F. Marone, D. Giardini, S. van der Lee, Seismic evidence for water deep in Earth's upper mantle. *Science* **300**, 1556–1558 (2003).
14. J. Revenaugh, S. Sipkin, Seismic evidence for silicate melt atop the 410-km mantle discontinuity. *Nature* **369**, 474–476 (1994).
15. T.-R. A. Song, D. V. Helmberger, S. P. Grand, Low-velocity zone atop the 410-km seismic discontinuity in the northwestern United States. *Nature* **427**, 530–533 (2004).
16. H. S. C. O'Neill *et al*., Mössbauer spectroscopy of mantle transition zone phases and determination of minimum Fe^{3+} content. *Am. Mineral.* **78**, 456–460 (1993).
17. D. J. Frost *et al*., Experimental evidence for the existence of iron-rich metal in the Earth's lower mantle. *Nature* **428**, 409–412 (2004).
18. A. Rohrbach *et al*., Metal saturation in the upper mantle. *Nature* **449**, 456–458 (2007).
19. H. Mao, P. Bell, "Disproportionation equilibrium in iron-bearing systems at pressures above 100 kbar with applications to chemistry of the Earth's mantle" in *Energetics of Geological Processes*, S. K. Saxena, S. Bhattacharji, H. Annersten, O. Stephansson, Eds. (Springer, 1977), pp. 236–249.
20. D. J. Frost, C. A. McCammon, The redox state of Earth's mantle. *Annu. Rev. Earth Planet. Sci.* **36**, 389–420 (2008).
21. F. Kaminsky, Mineralogy of the lower mantle: A review of 'super-deep'mineral inclusions in diamond. *Earth Sci. Rev.* **110**, 127–147 (2012).
22. E. M. Smith *et al*., Large gem diamonds from metallic liquid in Earth's deep mantle. *Science* **354**, 1403–1405 (2016).
23. T. Suzuki, S.-i. Akimoto, Y. Fukai, The system iron-enstatite-water at high pressures and temperatures—Formation of iron hydride and some geophysical implications. *Phys. Earth Planet. Inter.* **36**, 135–144 (1984).
24. T. Okuchi, Hydrogen partitioning into molten iron at high pressure: Implications for Earth's core. *Science* **278**, 1781–1784 (1997).
25. Y. Shibazaki, E. Ohtani, H. Terasaki, A. Suzuki, K.-i. Funakoshi, Hydrogen partitioning between iron and ringwoodite: Implications for water transport into the Martian core. *Earth Planet. Sci. Lett.* **287**, 463–470 (2009).
26. R. Iizuka-Oku *et al*., Hydrogenation of iron in the early stage of Earth's evolution. *Nat. Commun.* **8**, 14096 (2017).
27. E. Ito, T. Katsura, A temperature profile of the mantle transition zone. *Geophys. Res. Lett.* **16**, 425–428 (1989).
28. T. Katsura, E. Ito, The system Mg_2SiO_4-Fe_2SiO_4 at high pressures and temperatures: Precise determination of stabilities of olivine, modified spinel, and spinel. *J. Geophys. Res. Solid Earth* **94**, 15663–15670 (1989).
29. S. D. Jacobsen, S. Demouchy, D. J. Frost, T. B. Ballaran, J. Kung, A systematic study of OH in hydrous wadsleyite from polarized FTIR spectroscopy and single-crystal X-ray diffraction: Oxygen sites for hydrogen storage in Earth's interior. *Am. Mineral.* **90**, 61–70 (2005).
30. V. Clesi *et al*., Low hydrogen contents in the cores of terrestrial planets. *Sci. Adv.* **4**, e1701876 (2018).
31. K. Hirose *et al*., Hydrogen limits carbon in liquid iron. *Geophys. Res. Lett.* **46**, 5190–5197 (2019).
32. S. A. Peacock, Fluid processes in subduction zones. *Science* **248**, 329–337 (1990).
33. J. E. Dixon, L. Leist, C. Langmuir, J.-G. Schilling, Recycled dehydrated lithosphere observed in plume-influenced mid-ocean-ridge basalt. *Nature* **420**, 385–389 (2002).
34. R. J. Bodnar *et al*., "Whole Earth geohydrologic cycle, from the clouds to the core: The distribution of water in the dynamic Earth system" *Geological Society of America Special Papers*, M. E. Bickford, Ed. (Geological Society of America, 2013), vol. 500, pp. 431–461.
35. S.-i. Karato, Water distribution across the mantle transition zone and its implications for global material circulation. *Earth Planet. Sci. Lett.* **301**, 413–423 (2011).
36. M. Gurnis, C. Hall, L. Lavier, Evolving force balance during incipient subduction. *Geochem. Geophys. Geosyst.* **5**, Q07001 (2004).
37. O. Tschauner *et al*., Ice-VII inclusions in diamonds: Evidence for aqueous fluid in Earth's deep mantle. *Science* **359**, 1136–1139 (2018).
38. Q. Hu *et al*., FeO_2 and FeOOH under deep lower-mantle conditions and Earth's oxygen-hydrogen cycles. *Nature* **534**, 241–244 (2016).
39. J. Liu *et al*., Hydrogen-bearing iron peroxide and the origin of ultralow-velocity zones. *Nature* **551**, 494–497 (2017).
40. K. Sakamaki *et al*., Melting phase relation of FeH_x up to 20 GPa: Implication for the temperature of the Earth's core. *Phys. Earth Planet. Inter.* **174**, 192–201 (2009).
41. K. D. Leinenweber *et al*., Cell assemblies for reproducible multi-anvil experiments (the COMPRES assemblies). *Am. Mineral.* **97**, 353–368 (2012).
42. Y. Kudoh, T. Inoue, H. Arashi, Structure and crystal chemistry of hydrous wadsleyite, $Mg_{1.75}SiH_{0.5}O_4$: Possible hydrous magnesium silicate in the mantle transition zone. *Phys. Chem. Miner.* **23**, 461–469 (1996).
43. H. K. Mao, W. A. Bassett, T. Takahashi, Effect of pressure on crystal structure and lattice parameters of iron up to 300 kbar. *J. Appl. Phys.* **38**, 272–276 (1967).
44. C. Prescher, V. B. Prakapenka, DIOPTAS: A program for reduction of two-dimensional X-ray diffraction data and data exploration. *High Press. Res.* **35**, 223–230 (2015).
45. Y. Seto, D. Nishio-Hamane, T. Nagai, N. Sata, Development of a software suite on X-ray diffraction experiments. *The Review of High Pressure Science and Technology* **20**, 269–276 (2010).